

CHARACTERISTICS, AFFINITIES AND AGES OF VOLCANIC DEPOSITS ASSOCIATED WITH THE ORIENTALE BASIN FROM CHANDRAYAAN-1 MOON MINERALOGY MAPPER (M3) DATA: MARE STRATIGRAPHY. J. Head¹, M. Staid², C. Pieters¹, J. Mustard¹, L. Taylor³, T. McCord⁴, P. Isaacson¹, R. Klima¹, J. Nettles¹, J. Whitten¹, and the M3 Team. ¹Brown Univ., Providence RI 02912; ²PSI, Tucson AZ; ³Univ. Tenn., Knoxville TN 37996; ⁴BFC, Winthrop, WA; (james_head@brown.edu).

Introduction and Background: The ~930 km diameter Orientale basin, the youngest and most well preserved multi-ringed basin on the Moon, displays a remarkably fresh and very sparsely flooded basin interior [1-3]. Orientale provides a background template on which to analyze and assess the locations, ages, volumes, mineralogies and modes of emplacement of volcanic deposits associated with the basin. Deposits of volcanic origin associated with the Orientale basin have six main modes of occurrence: 1) Mare Orientale itself, occurring in the central part of the basin, covering 47,000 km², and estimated to be ~1 km thick [1]; 2) Lacus Veris and Lacus Autumni, consisting of small lava ponds arranged in arcuate bands in the northeast part of the basin at the base of the Outer Rook and Cordillera Mountains respectively [4]; 3) the dark ring to the south of Orientale [5-7]; 4) cryptomaria in regions generally distal to the Orientale basin ejecta deposit (the Hevelius Formation and adjacent smooth plains) [8-11], 5) mare deposits on the floors of post-Orientale impact craters such as Schlüter [4], and 6) post-Orientale deposits that lap onto distal basin deposits and that often occur in the vicinity of cryptomaria [10]. We use a mosaic of images at ~155 m/pxl (2.9 μm; reflected light and thermal emission) and spectra from the Moon Mineralogy Mapper (M3) experiment [12] flown onboard Chandrayaan-1 to define and characterize the array of volcanic deposits, focusing on mare stratigraphy and building on numerous previous studies of volcanism in the Orientale region.

Background, Ages and Stratigraphy: Observations from Earth are limited due to the position of Orientale on the western limb, but Earth-based telescopic data reported by Hawke et al. [13] indicated a titanium content for Lacus Veris and Lacus Autumni that they interpreted to be similar to that of central Mare Serenitatis. Greeley et al. [9] used Galileo Solid State Imaging (SSI) experiment data to analyze the maria in Orientale and related areas. For the mare deposits, ratios of 0.41-0.56 μm filter images provided information on the titanium content, and 0.76/0.99 ratios indicated 1 μm absorptions related to Fe²⁺ in mafic minerals. These data, together with stratigraphic relations determined in images and crater-size frequency distribution data from Lunar Orbiter images, provided a first synthesis of the history and mineralogy of the modification of the Orientale basin by mare deposits (Fig. 1). The oldest mare materials detected in the Orientale basin interior (~3.7 Ga old) occur in the south-central part of the basin, and the youngest [11] occur in Lacus Autumni (~2.85 Ga

old), along the base of the Cordillera Mountain ring. Kadel et al. [14] reported even younger basalts in central Lacus Veris (~2.29 Ga). Thus, on the basis of these data, volcanic activity in the Orientale interior spans ~0.85 Ga (or possibly 1.41 Ga [14]), starting ~100 Ma after basin formation. Subsequent to the earliest maria (~3.70 Ga), additional mare deposits were emplaced in western and southeastern Mare Orientale at about 3.45 Ga. The maria within Mare Orientale are medium to medium-high titanium (<4-7% TiO₂), with the lower Ti signatures in the northeastern and west central Mare Orientale being attributed to contamination of the deposits by Orientale basin (highland) material ejected by the Hohmann Q and Maunder impacts. Lacus Veris crater counts yield an age of 3.50 Ga and the SSI data yield evidence for a medium-high-titanium soil. The outermost mare deposits within the basin, Lacus Autumni, were dated at 3.4 Ga and 2.85 Ga [14], and medium-high-titanium soils in the north and medium-titanium soils in the south, the latter possibly due to contamination from adjacent highlands [9]. These results are consistent with Earth-based measurements [13]. Greeley et al. [9] conclude that although mare volcanic activity spans at least 0.85 Ga in duration, the mare deposits display a fairly narrow range of compositions relative the much wider diversity seen in nearside mare deposits (e.g., Hiesinger et al. [15-17]).

New Mare Deposits Detected by M3: Most previous work has focused on the distribution of mare patches in Lacus Veris and Autumni and hypothesized that the restriction of mare deposits outside Mare Orientale to this quadrant is related to gradients in crustal and/or lithospheric thickness [18-19]. The increased spatial and spectral resolution of M3, however, has revealed the presence of small mare ponds along the western and southern margins of the basin (Fig. 2). Two of these (Fig. 3) have been previously noted in Zond data [20-22], and form small ponds, one about 30 x 12 km on the back slope of the Outer Rook Mountains and the other, nearby at the base of the OR in a 65 x 20 km patch, is at the position of the Lacus Veris ponds in the northeast quadrant. The third patch (Fig. 4), ~8 x 15 km, lies just east of some of the innermost massifs of the Outer Rook ring and just west of the Inner Rook ring. The fourth patch (~12 km; Fig. 5) is superposed on smooth plains within the Montes Rook Formation and the fifth (~10 x 13 km; Fig. 6) lies at the margin of the Montes Rook and the Hevelius Formation. These patches lie near the base of the outer Cordillera ring, in a position similar to mare ponds comprising Lacus Autumni in the northeast quadrant. Although these new deposits are relatively small compared to other patches of

maria [4], nonetheless they illustrate that magma was reaching the surface throughout this region over a much broader area than previously thought. Although too small to yield robust crater-age dates, we are currently assessing the spectral characteristics of these western patches in order to compare their affinities to those elsewhere in Orientale (Fig. 1,2).

Conclusions: Stratigraphic relationships and ages show that: 1) mare filling began ~100 Ma after basin formation in the basin interior followed by activity in Lacus Veris, then a second phase in the interior, followed by Lacus Autumni, and possibly latest activity in Lacus Veris, with a total duration of 0.85-1.41 Ga [9,14], but relatively low total volumes [4]. 2) Eruption locations were focused in the interior and along the

outer two basin rings; M3 data show that activity was widespread within the basin, but concentrated in the interior and northeast quadrant.

References: 1. J. Head, Moon 11, 327, 1974; 2. K. Howard et al., RGSP 12, 309, 1974; 3. J. McCauley, PEPI 15, 220, 1977; 4. A. Yingst & J. Head, JGR 102, 10909, 1997; 5. P. Schultz & P. Spudis, LPS 9, 1033, 1978; 6. C. Weitz et al., JGR 103, 22725, 1997; 7. J. Head et al., JGR 107, JE001438, 2002; 8. P. Schultz and P. Spudis, PLSPC 10, 2899, 1979; 9. R. Greeley et al., JGR 98, 78183, 1993; 10. J. Mustard & J. Head, JGR 101, 18913, 1996; 11. D. Williams et al., JGR, 100, 23291, 1995; 12. C. Pieters et al., Current Science 96, 500, 2009; 13. B. Hawke et al., GRL 18, 2141, 1991; 14. S. Kadel et al., LPSC 24 745, 1993; 15. H. Hiesinger et al., JGR 108, 5065, 2003; 16. H. Hiesinger et al., JGR JE003380, 2009; 17. H. Hiesinger et al., JGR 105, 29239, 2000; 18. S. Solomon & J. Head, RGSP 18, 107, 1980; 19. J. Head & L. Wilson, G&CA 56, 2155, 1992; 20. D. Scott et al., USGS Map 1-1034, 1977; 21. Y. Lipsky et al., Kosm. Issled. 4, 912, 1966; 22. J. Head et al., JGR 98, 17149, 1993.

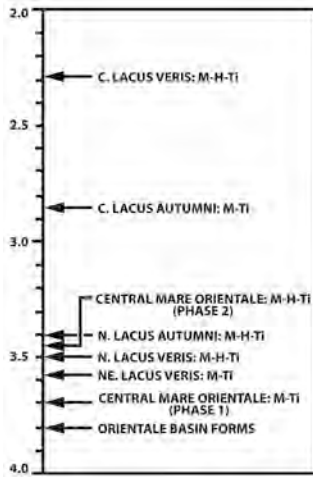


Fig. 1. Phases in the emplacement of mare deposits in Ga following the formation of the Orientale basin at 3.8 Ga. From [9, 14].

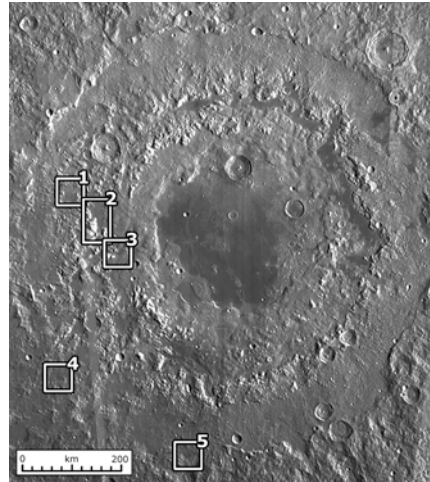


Fig. 2. Location of five mare deposits in the western part of the Orientale basin unrelated to Mare Orientale or Lacus Veris and Autumnae, and mapped in M3 data (see Figs. 3-6). Base is mosaic of M3 data at 2.9 μm .

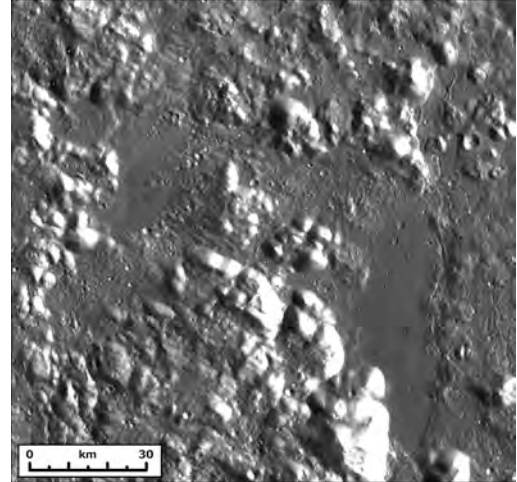


Fig. 3. Mare patches 1 and 2 (Fig. 2).

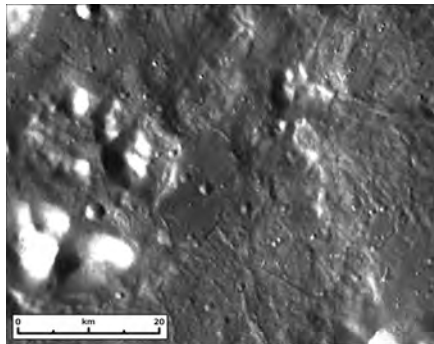


Fig. 4. Mare patch 3 (Fig. 2).

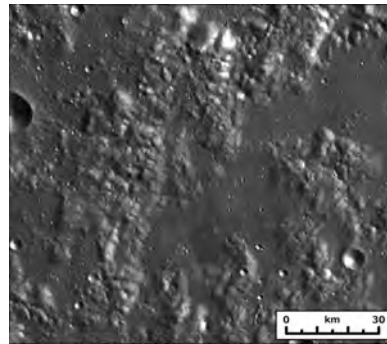


Fig. 5. Mare patch 4 (Fig. 2).

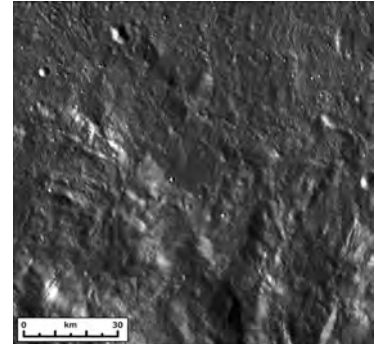


Fig. 6. Mare patch 5 (Fig. 2).